

Paper:

# Estimation of a Source Model and Strong Motion Simulation for Tacna City, South Peru

Nelson Pulido<sup>\*1</sup>, Shoichi Nakai<sup>\*2</sup>, Hiroaki Yamanaka<sup>\*3</sup>, Diana Calderon<sup>\*4</sup>,  
Zenon Aguilar<sup>\*4</sup>, and Toru Sekiguchi<sup>\*2</sup>

<sup>\*1</sup>National Research Institute for Earth Science and Disaster Prevention

3-1 Tennodai, Tsukuba, Ibaraki 305-0006, Japan

E-mail: nelson@bosai.go.jp

<sup>\*2</sup>Chiba University, Chiba, Japan

<sup>\*3</sup>Tokyo Institute of Technology, Kanagawa, Japan

<sup>\*4</sup>Universidad Nacional de Ingeniería, Perú, Lima, Perú

[Received August 18, 2014; accepted September 8, 2014]

We estimate several scenarios for source models of megathrust earthquakes likely to occur on the Nazca-South American plates interface in southern Peru. To do so, we use a methodology for estimating the slip distribution of megathrust earthquakes based on an interseismic coupling (ISC) distribution model in subduction margins and on information about historical earthquakes. The slip model obtained from geodetic data represents large-scale features of asperities within the megathrust that are appropriate for simulating long-period waves and tsunami modelling. To simulate broadband frequency strong ground motions, we add small scale heterogeneities to the geodetic slip by using spatially correlated random noise distributions. Using these slip models and assuming several hypocenter locations, we calculate a set of strong ground motions for southern Peru and incorporate site effects obtained from microtremors array surveys in Tacna, the southernmost city in Peru.

**Keywords:** strong motion, source process, 1868 earthquake, seismic hazard, South Peru

## 1. Introduction

To improve seismic hazard assessment of rare megathrust earthquakes such as the Sumatra 2004, Chile 2010, and Japan 2011 earthquakes, it may be useful to incorporate information on crustal deformation at plate margins. The development of global positioning systems (GPS) and satellite radar interferometry (InSAR) have made it possible to measure strain buildup associated with plate coupling in many earthquake-prone regions worldwide [1]. Recent studies suggest that subducting plates are either locked or creeping aseismically and that a patchwork of locked or coupled regions during the interseismic period may be related to asperities in earthquakes [2–4]. We apply a methodology for characterizing source models of megathrust earthquakes based on the interseismic coupling (ISC) spatial distribution of subduc-

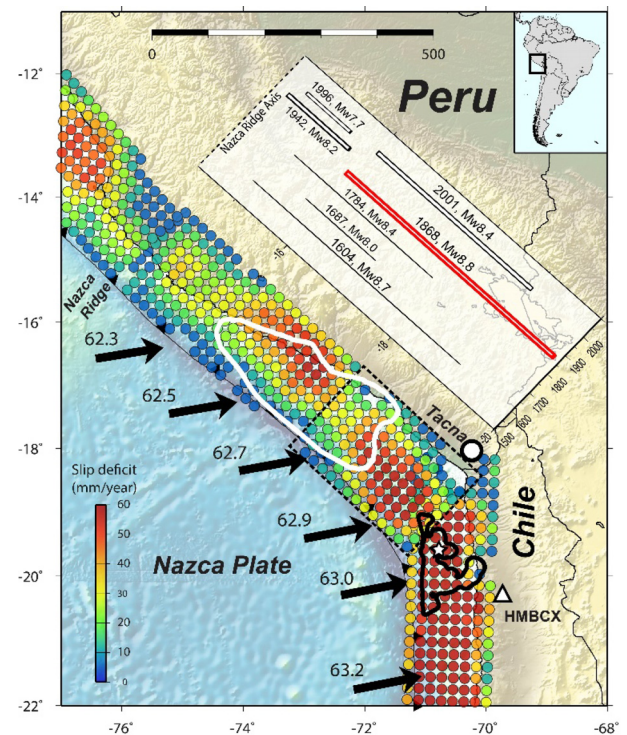


**Fig. 1.** Slip deficit in southern Peru and northern Chile obtained from geodetic measurements and historical earthquakes along the Nazca subduction zone in Peru [1]. Black arrows are velocity vectors for the Nazca Plate at the margin convergence with the South American Plate [1]. The dashed black line encloses the source area of our scenario earthquakes in southern Peru. The continuous white line encloses the source area of the 2001 Arequipa earthquake, Peru ( $M_w$ 8.4) [1]. The continuous black line encloses the source area of the 2014 Iquique earthquake, Chile ( $M_w$ 8.2) [8]. The white dashed line encloses the source area of the 1877 earthquake in northern Chile. The location of the HMBCX strong motion station in Chile is shown by a triangle.

tion zones and information on historical earthquakes [5] to southern Peru, which is a very active seismic region characterized by the fast subduction of the Nazca plate beneath the South American plate (**Fig. 1**). Seismic activity

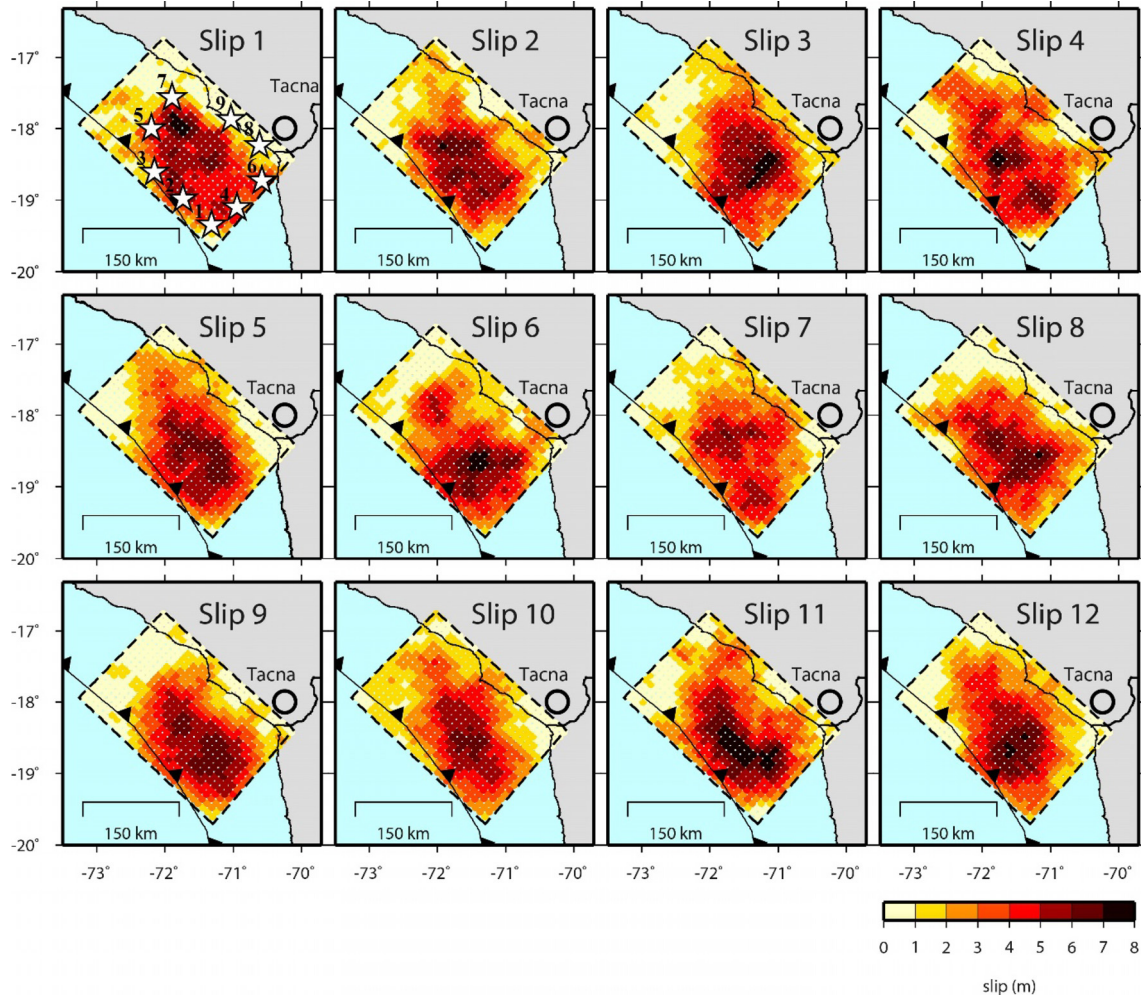


**Fig. 2.** Broadband source models constructed by adding short wavelength slip distributions obtained from a Von Karman power spectral density (PSD) function with random phases to the slip model inferred from geodetic data for southern Peru. The panel corresponding to slip No.1 shows the 9 starting points of rupture used for our scenarios.

in Peru is divided by the Nazca ridge (15°S) into two regions, north or south of the ridge. The ridge is coincident with a region of low coupling where the Nazca plate is believed to subduct aseismically [1, 2] and therefore possibly act as a geomorphological barrier to seismic rupture propagation. Southern Peru has been repeatedly affected by large earthquakes such as the great 1868 earthquake, which had a moment magnitude of ~8.8 [6]. In 2001, the Arequipa earthquake, which measured  $M_w$ 8.4, released a large fraction of slip accumulated in the region since the 1868 event (**Fig. 1**). We use this information combined with an ISC model of central and southern Peru to construct possible scenarios for the next megathrust earthquake that would likely affect Tacna, the southernmost city in Peru.

## 2. Source Models for Central and Southern Peru

### 2.1. ISC Model and Scenario Earthquakes

An ISC model in Peru was obtained by inverting velocities from GPS campaigns at 87 sites surveyed from 1993 to 2003 [1]. The model for ISC assumes that con-

vergence between the Nazca and South American plates is dominantly accommodated along the megathrust, including 4mm/year of back-arc shortening absorbed in the sub-Andean fold and thrust belt regions [1]. ISC results indicate the existence of two strongly coupled regions – the first near the source of the Arequipa earthquake (white contour line in **Fig. 1**) and the second near Tacna. **Fig. 1** shows the slip deficit rate, obtained by multiplying the ISC distribution by the plate convergence rate proposed in [7]. In southern Peru, we assume that the interseismic process has stood since the 1868 earthquake. Removing the slip released by the Arequipa earthquake in 2001 ( $M_w$ 8.4) results in an earthquake scenario with a moment magnitude of 8.5. We place a southern limit for our scenario fault model at the bend of the Nazca plate, near the border region between Peru and Chile, the source area enclosed by the black dashed line in **Fig. 1**. A large subduction earthquake occurred in the northern Chile region in April 2014 ( $M_w$ 8.2) [8], and this probably released a large fraction of the slip accumulating in north Chile since the 1877 earthquake (**Fig. 1**), providing an additional constraint for a possible fault rupture further south of the bend.

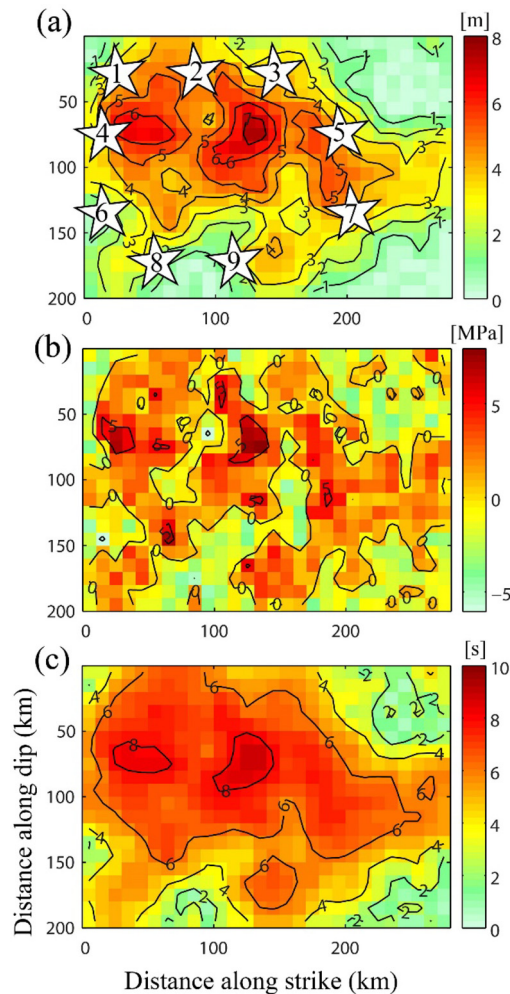


**Fig. 3.** a) Slip, b) Stress drop, c) Rise time distributions across the fault plane for the slip scenario in southern Peru (slip No.4 in Fig. 2). The 9 starting points of rupture are shown by white stars.

## 2.2. Slip Scenario Earthquakes

The fault dimensions of our source models for southern Peru are 280 km (along strike) by 200 km (along dip) (Fig. 1). This model features a smooth distribution of asperities partly due to the large grid spacing used to estimate the ISC model (20 km) (Fig. 1). This model is appropriate for simulating long-period seismic waves and for tsunami modelling. For simulating a strong broadband ground motion, we introduce small-scale complexities into the source slip to simulate high-frequency ground motion, for which we construct a “broadband” source model in which large-scale features of the slip are obtained from the ISC model and short wavelength slip distribution is obtained from spatially correlated random noise [5]. To calculate a set of broadband slip scenarios based on the ISC to be used for strong motion simulation, we calculated a set of 12 short wavelength slip models and added them to the long wavelength slip. The 12 broadband slip models used for strong motion simulation are shown in Fig. 2. Slip distributions have been obtained for a subfault size of 10 km.

**Table 1.** Parameters for strong motion simulation.

| Parameter                                     | Value                                |
|---|--------------------------------------|
| Grid size (km)                                | 10                                   |
| Subfaults along strike, dip                   | 28, 20                               |
| Sampling period (s)                           | 0.01                                 |
| Strike/Dip/Rake (degrees)                     | 313/20/54.6                          |
| Stress drop distribution                      | from slip model                      |
| Rise time distribution                        | from slip model                      |
| Rupture velocity (km/s)                       | 2.87                                 |
| Radiation pattern frequencies $f_1, f_2$ (Hz) | 1, 5 (Palido and Dalguer 2009)       |
| $f_{\max}$ (Hz)                               | 10                                   |
| Average S-wave velocity (km/s)                | 3.99                                 |
| Average density ( $T/m^3$ )                   | 3.0                                  |
| Anelastic attenuation (Q)                     | $210f^{0.7}$ (Raouf and Nutti, 1984) |
| Geometrical spreading                         | Garcia et al. 2009                   |

## 3. Strong Motion Simulation Method and Parameters

To perform strong motion simulation, we used a hybrid methodology [5, 9] that combines the deterministic simulation of ground motion at low frequencies with semistochastic simulation at high frequencies and assume a flat-layered 1D velocity structure. Broadband simulation for the present study is performed in the 0.05 Hz–30 Hz frequency range. The methodology has been extensively tested and validated in previous studies [9–14]. To calculate strong motion simulation for the Tacna region, we used the 12 broadband slip source models obtained as detailed in the previous section and assumed 9 different locations for starting points of the rupture (white stars in Fig. 3a), yielding 108 fault rupture scenarios. Hypocenter locations were determined based on [15], indicating that earthquakes ruptures tend to nucleate close to large slip regions. The main parameters for simulation are slip, stress drop, and rise time distribution across the fault plane and rupture velocity (Fig. 3 and Table 1).

## 4. Velocity Models and Strong Motion Simulations in Tacna

In Tacna, we calculated the EW, NS, and UD components of strong ground motions at the 8 points shown in Fig. 5 for a seismic bedrock condition of  $V_s = 2790$  m/s. Crustal velocity models for these calculations (Table 2) were obtained by combining results from P and S wave seismic tomography from a regional deployment of 18 seismic stations [16] and P-wave tomography and receiver function analysis from a linear array deployment of 50 broadband seismic stations in southern Peru [17]. We calculated accelerograms at the surface by performing convolution between seismic bedrock waveforms with soil transfer functions at the 8 points in Fig. 5. Deep soil velocity models up to 1 km deep were obtained

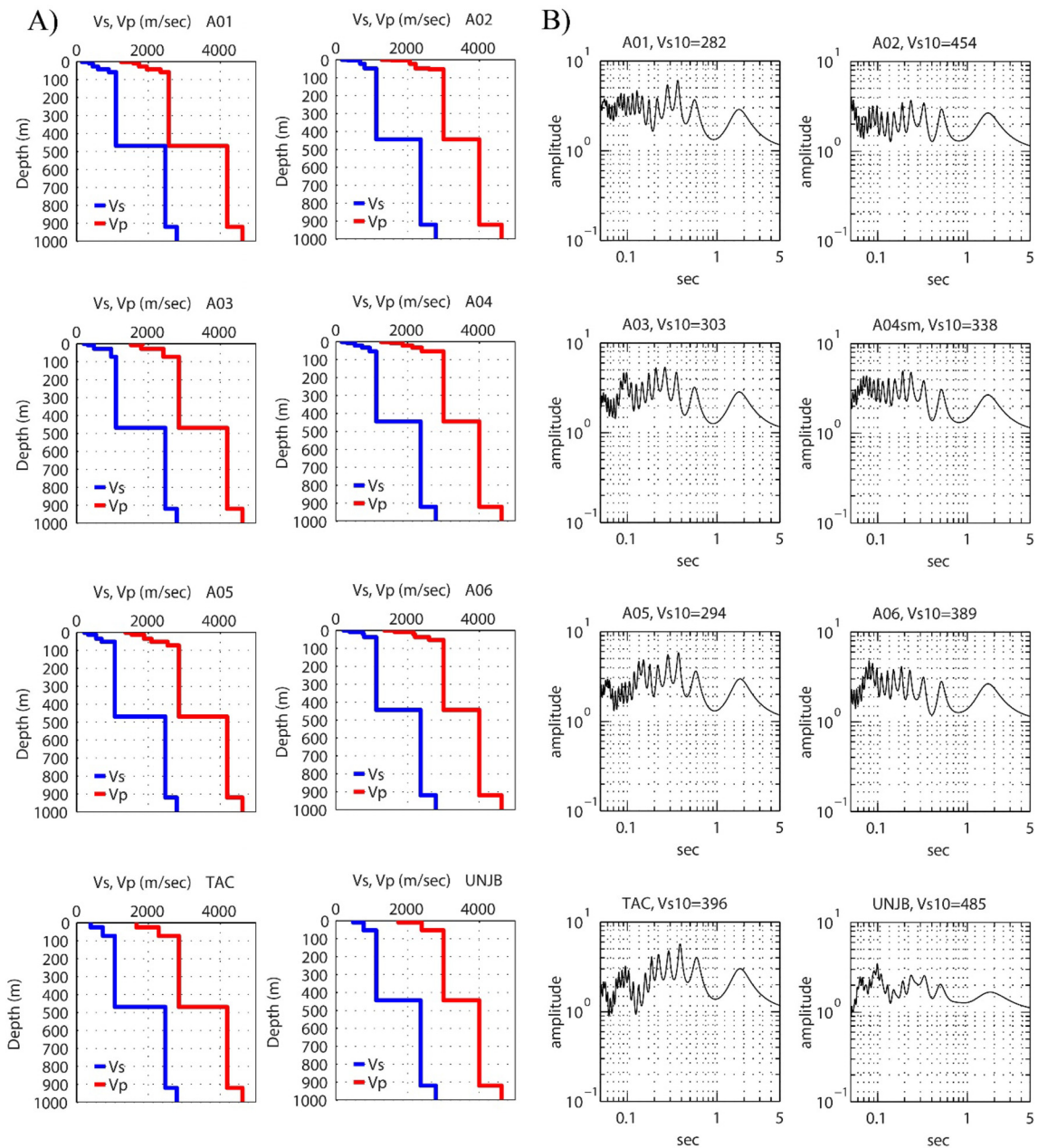


**Fig. 4.** a) Velocity models from seismic bedrock ( $V_s = 2790$  m/s) up to the surface at 8 sites in Tacna obtained from array microtremor measurement [18]. See site locations in **Fig. 5.** b) Transfer functions for velocities in a).

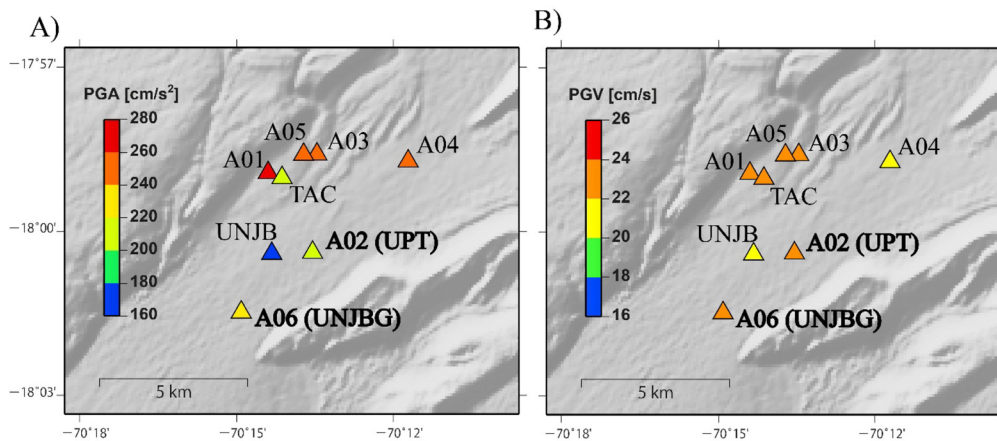


**Fig. 5.** a) Average PGA distributions in Tacna for all scenarios in southern Peru. b) Same for PGVs. Values incorporate shallow site effects.

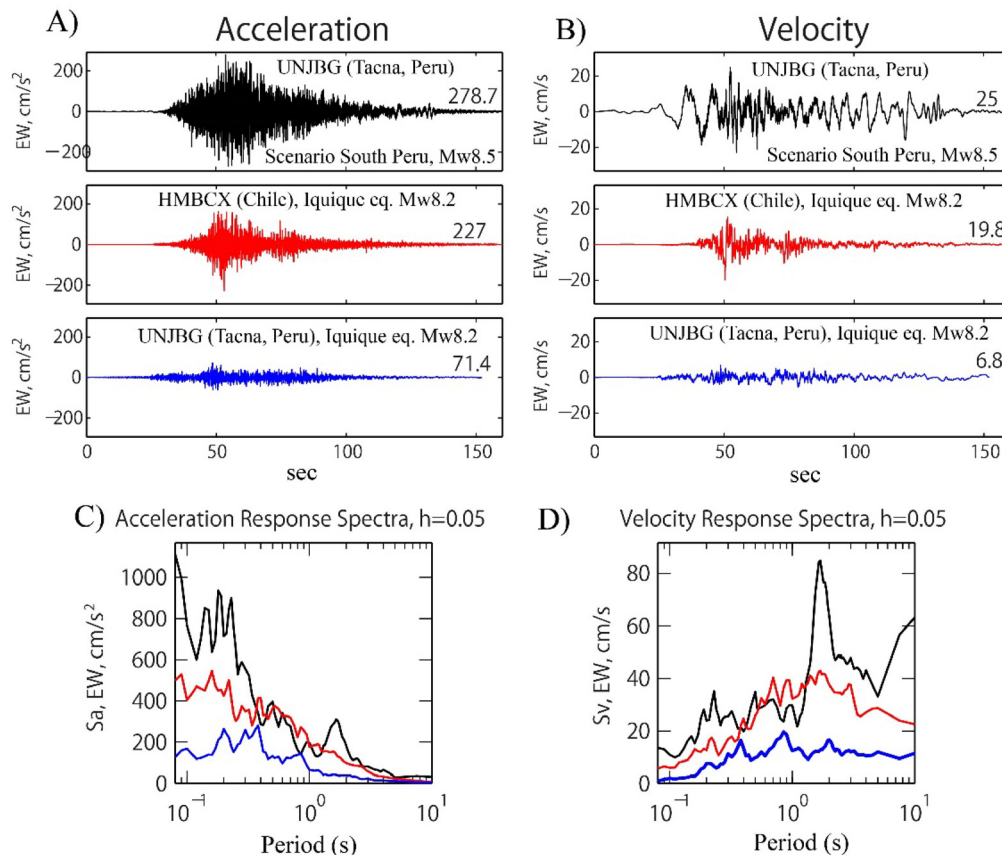


**Fig. 6.** a) Simulated accelerogram in Tacna (UNJBG station) for a scenario earthquake in southern Peru (Slip No.4, hypocenter 1 in Fig. 3) (black line). The red line is the observed accelerogram of the April 1, 2014, Iquique earthquake, North Chile ( $M_w$ 8.2) at the HMBCX strong motion station in Chile. The blue line is the observed accelerogram of the Iquique earthquake in Tacna (UNJBG station). b) Velocity waveforms of records in a). Acceleration and velocity response spectra for all waveforms are shown in c) and d) using the same color code.

**Table 2.** Velocity model of southern Peru.

| Depth (km) | $V_p$ (m/s) | $V_s$ (m/s) | density ( $kg/m^3$ ) | $Q_p$ | $Q_s$ |
|------------|-------------|-------------|----------------------|-------|-------|
| 0          | 4620        | 2790        | 2479                 | 513   | 257   |
| 5          | 5800        | 3500        | 2675                 | 784   | 392   |
| 20         | 7120        | 4200        | 3003                 | 1171  | 585   |
| 36         | 7700        | 4390        | 3187                 | 1301  | 650   |
| 88         | 8000        | 4613        | 3291                 | 1469  | 734   |

$V_p$  and  $V_s$  values from Cunningham et al. (1986), and Phillips et al. (2012) other parameters obtained from  $V_p$  using empirical scalings by Brocher et al. (2008).

from microtremor array measurement at TAC and UNJB sites [18]. Shallow soil velocity models up to 100 m were obtained from array measurement by CISMID at six additional sites (A01 to A06) (Figs. 4 and 5). Our simulated average PGA and PGV values at these sites for all scenarios are 160 ~ 280  $cm/s^2$  and 20 ~ 24  $cm/s$ . These values are approximately 3 times smaller than simulated values in Lima for an earthquake scenario with a moment magnitude of 8.9 [5], mainly due to the greater distance that Tacna is from the source area than Lima and the smaller

magnitude of the southern Peru scenario compared to the scenario in Central Peru [5]. Fig. 6 (black line) shows the simulated EW accelerogram in Tacna at the UNJBG strong motion station location (Fig. 5) for the scenario earthquake in southern Peru (Slip No.4, Hypocenter 1 in Fig. 2). The red line is the observed accelerogram of the April 1, 2014, Iquique earthquake in north Chile ( $M_w$ 8.2), at the HMBCX strong motion station (Fig. 1). The blue line is the observed accelerogram of the Iquique earthquake in Tacna (UNJBG station). Note that the amplitude of simulated strong motion of our scenario for southern Peru is comparable to observed values for the Iquique earthquake at HMBCX station for similar slip centroid distances of 130 km vs 100 km and magnitudes  $M_w$ 8.5 vs  $M_w$ 8.2 (Fig. 6).

Although our selection of the number of broadband slips and rupture models is arbitrary (108), we consider that these scenarios generate a wide range of ground motion for the megathrust earthquake likely to occur in southern Peru as discussed in Section 2.1. We cannot rule out the possibility that more critical scenarios in ground shaking for Tacna could be obtained from a 1868 type earthquake or other types of tectonic sources such as active faults, but that is beyond the scope of this study.

## 5. Conclusions

We applied a methodology for estimating slip scenarios for megathrust earthquakes combining models of ISC distribution in subduction margins obtained from geodetic data, information on historical earthquakes, and spatially correlated random noise distribution representing small scale heterogeneities of slip in the southern Peru region. Our results for southern Peru suggest an earthquake scenario with a moment magnitude of  $M_w = 8.5$ , a source rupture area of approximately 280 km (along strike) and 200 km (along dip). Our strong motion simulation results for Tacna show values of PGA and PGV of approximately 240  $\text{cm/s}^2$  and 22  $\text{cm/s}$ , which are much smaller than strong motion simulation values for Lima for a scenario earthquake in central Peru ( $M_w 8.9$ ) [5]. This difference can be explained because of the smaller magnitudes of the scenarios for Tacna as compared to scenarios for Lima, as well as the larger fault-distance for Tacna as compared to Lima. Amplitudes of the simulated strong motion of our scenario for southern Peru ( $M_w 8.5$ ) are comparable to values observed for the 2014 Iquique earthquake ( $M_w 8.2$ ) for a similar source distance.

### Acknowledgements

This study was supported by the SATREPS project Enhancement of Earthquake and Tsunami Mitigation Technology in Peru. We thank Fernando Lazares, CISMID, Peru, and Chile University (IPOC network) for kindly providing strong motion records for the Iquique earthquake in the UNJBG station in Tacna and the HMBCX station in north Chile.

### References:

- [1] M. Chlieh, H. Perfettini, H. Tavera, J.-P. Avouac, D. Remy, J.-M. Nocquet, et al., "Interseismic coupling and seismic potential along the Central Andes subduction zone," *J. Geophys. Res.*, 116, B12405, doi:10.1029/2010JB008166, 2011.
- [2] H. Perfettini, J.-P. Avouac, H. Tavera, A. Kositsky, J.-M. Nocquet, F. Bondoux, M. Chlieh, A. Sladen, L. Audin, D. Farber, and P. Soler, "Aseismic and seismic slip on the Megathrust offshore southern Peru revealed by geodetic strain before and after the  $M_w 8.0$ , 2007 Pisco earthquake," *Nature*, Vol.465, pp. 78-81, doi:10.1038/nature09062, 2010.
- [3] N. Moreno, M. Rosenau, and O. Oncken, "2010 Maule earthquake slip correlates with pre-seismic locking of Andean subduction zone," *Nature*, 467, pp. 198-204, 2010.
- [4] J. P. Loveless and B. J. Meade, "Spatial correlation of interseismic coupling and coseismic rupture extent of the 2011  $M_w = 9.0$  Tohoku-oki earthquake," *Geophys. Res. Lett.*, Vol.38, No.17, doi: 10.1029/2011GL048561, 2011.
- [5] N. Pulido, Z. Aguilar, H. Tavera, M. Chlieh, D. Calderon, T. Sekiguchi, S. Nakai, and F. Yamazaki, "Scenario source models and strong ground motion for future mega-earthquakes: Application to Lima, Central Peru," *Bull. Seism. Soc. Am.*, 2014 (in press).
- [6] L. Dorbath et al., "Assessment of the size of large and great historical earthquakes in Peru," *Bull. Seismol. Soc. Am.*, Vol.80, No.3, pp. 551-576, 1990.
- [7] E. Kendrick, M. Bevis, J. R. Smalley, B. Brooks, R. B. Vargas, E. Lauria et al., "The Nazca-South America Euler vector and its rate of change," *J. South Am. Earth Sci.*, Vol.16, No.2, pp. 125-131, doi:10.1016/S0895-9811(1003)00028-00022, 2003.
- [8] W. Suzuki, N. Pulido, and S. Aoi, "Rupture process of the 2014 Northern Chile (Pisagua) earthquake derived from strong-motion records," *Proceedings of the 14<sup>th</sup> Japan Earthquake Engineering Symposium*, 2014 (in press).
- [9] N. Pulido and T. Kubo, "Near-Fault Strong Motion Complexity of the 2000 Tottori Earthquake (Japan) from a Broadband Source Asperity Model," *Tectonophysics*, Vol.390, pp. 177-192, 2004.

- [10] N. Pulido, A. Ojeda, K. Atakan, and T. Kubo, "Strong Ground Motion Estimation in the Marmara Sea Region (Turkey) Based on a Scenario Earthquake," *Tectonophysics*, Vol.391, pp. 357-374, 2004.
- [11] M.. B. Sorensen, K. Atakan, and N. Pulido, "Simulated strong ground motions for the great M9.3 Sumatra-Andaman earthquake of December 26, 2004," *Bull. Seism. Soc. Am.*, Vol.97, No.1A, pp. S139-S151, doi: 10.1785/0120050608, 2007a.
- [12] M.. B. Sorensen, N. Pulido, and K. Atakan, "Sensitivity of Ground-Motion Simulations to Earthquake Source Parameters: A Case Study for Istanbul, Turkey," *Bull. Seism. Soc. Am.*, Vol.97, pp. 881-900, doi: 10.1785/0120060044, 2007b.
- [13] N. Pulido and L. Dalguer, "Estimation of the high-frequency radiation of the 2000 Tottori (Japan) earthquake based on a dynamic model of fault rupture: Application to the strong ground motion simulation," *Bull. Seism. Soc. Am.*, Vol.99, No.4, pp. 2305-2322, doi: 10.1785/012008016, 2009.
- [14] N. Pulido, H. Tavera, Z. Aguilar, S. Nakai, and F. Yamazaki, "Strong Motion Simulation of the M8.0 August 15, 2007, Pisco Earthquake; Effect of a Multi-Frequency Rupture Process," *Journal of Disaster Research*, Vol.8, No.2, pp. 235-242, 2013.
- [15] P. M. Mai, P. Spudich, and J. Boatwright, "Hypocenter Locations in Finite-Source Rupture Models," *Bull. Seism. Soc. Am.*, Vol.95, pp. 965-980, doi: 10.1785/0120040111, 2005.
- [16] P. S. Cunningham, S. Roecker, and D. Hatzfeld, "Three-dimensional P and S wave velocity structures of southern Peru and their tectonic implications," *J. Geophys. Res.*, Vol.91, No.B9, pp. 9517-9532, 1986.
- [17] K. Phillips, R. W. Clayton, P. Davis, H. Tavera, R. Guy, S. Skinner, I. Stubaiko, L. Audin, and V. Aguilar, "Structure of the subduction system in southern Peru from seismic array data," *J. Geophys. Res.*, Vol.117, B11306, doi:10.1029/2012JB009540, 2012.
- [18] H.. Yamanaka, M. S. Quispe-Gamero, K. Chimoto, K. Saguchi, D. Calderon, F. Lazares, and Z. A. Bardales, "Exploration of Deep sedimentary layers in Tacna city, southern Peru, using microtremors and earthquake data for estimation of local amplification," *Journal of Seismology*, 2014 (in review).
- [19] T. Brocher, "Key elements of regional seismic velocity models for long period ground motion simulations," *J. Seismol.*, Vol.12, pp. 217-221, 2008.
- [20] D. Garcia, S. K. Singh, M. Herraiz, M. Ordaz, J. F. Pacheco, and H. Cruz-Jimenez, "Influence of subduction structure on coastal and inland attenuation in Mexico," *Geophys. J. Int.*, Vol.179, pp. 215-230, doi:10.1111/j.1365-246X.2009.04243.x, 2009.
- [21] M. Raouf and O. Nuttli, "Attenuation of High-Frequency Earthquake Waves in South America," *PAGEOPH*, Vol.122, pp. 619-644, 1984.



### Name:

Nelson E. Pulido H.

### Affiliation:

Senior Researcher, National Research Institute for Earth Science and Disaster Prevention (NIED)

### Address:

3-1, Tennodai, Tsukuba, Ibaraki 305-0006, Japan

### Brief Career:

2012- Senior Researcher, Earthquake and Volcano Research Unit, National Research Institute for Earth Science and Disaster Prevention (NIED), Japan

### Selected Publications:

- N. Pulido, Y. Yagi, H. Kumagai, and N. Nishimura, "Rupture process and coseismic deformations of the February 2010 Maule earthquake, Chile," *Earth, Planets and Space*, Vol.63, No.8, pp. 955-959, doi:10.5047/eps.2011.04.008, 2011.
- N. Pulido and L. Dalguer, "Estimation of the high-frequency radiation of the 2000 Tottori (Japan) earthquake based on a dynamic model of fault rupture: Application to the strong ground motion simulation," *Bull. Seism. Soc. Am.*, Vol.99, No.4, pp. 2305-2322, doi: 10.1785/012008016, 2009.

### Academic Societies & Scientific Organizations:

- American Geophysical Union (AGU)
- Seismological Society of America (SSA)
- Seismological Society of Japan (SSJ)
- Japan Association for Earthquake Engineering (JAEE)